Self-assembly in drying complex fluid at low capillary number

Ching Hsueh, Carmen Lucía Moraila Martínez, Frédéric Doumenc, Miguel Rodríguez-Valverde, Béatrice Guerrier

Self-assembly in Drying Complex Fluid

at Low Capillary Number

Ching Hsueh[a], Carmen Lucía Moraila Martínez[b], Frédéric Doumenc[a], Miguel A. Rodríguez-Valverde[b], Béatrice Guerrier[a]

[a] *UMPC Univ Paris 06, Univ Paris-Sud, CNRS, Lab FAST, Bat 502, Campus Univ, Orsay F-91405*

[b] *Department of Applied Physics, Faculty of Sciences, University of Granada, Granada, Spain*

ching@fast.u-psud.fr, cmoraila@ugr.es, doumenc@fast.u-psud.fr, marodri@ugr.es, guerrier@fast.u-psud.fr

Abstract

We study the pattern formation induced by drying colloidal suspensions and polymer solutions in a vertical Hele-Shaw cell immersed in a reservoir. The contact line speed is controlled by pumping out the solution from the reservoir. At low capillary number stick-slip motion of the receding contact line can be observed for silica suspensions. Periodic strips spontaneously form during drying. We study the strip periodicity and deposit morphology as a function of the receding velocity and pH of the solution. In the same conditions, dried polymer films are almost flat.

Keywords: silica nano-particles, stick-slip motion, dip-coating, pattern formation, drying

1. Introduction

Surface coating technologies used nowadays to fabricate nano-scale patterning is a main issue to investigate. Different methods are used to make patterned deposits: from the top-down point of view, photolithography and electron-beam lithography are well-developed. However, the parallelization and 2-D limitations are actual challenges. From the bottom-up point of view, self-assembly by evaporation is one of the promising ideas to fabricate nano-scale patterns [1-3]. Droplet drying has been widely investigated in fundamental studies [4-5] and for various applications, like biochemical ones [6]. Despite the simplicity of this geometry, its physical description remains quite complicated. Indeed the drying of a droplet is a non stationary phenomenon since its volume decreases while the non volatile solute concentration increases. In dip-coating configurations, also widely used in industrial coating processes, the concentration of the liquid bath remains constant so that a stationary phenomenon can be observed. Moreover, velocity can be controlled independently from evaporation. This configuration can then help to better describe and control the different phenomena that are exhibited in patterning.

Several regimes are encountered in dip-coating, depending on the capillary number. At high enough capillary number, the viscous forces dominate and the coating forms a continuous layer whose thickness is proportional to the substrate speed to the power 2/3 (Landau-Levich regime [7,8]). At lower speed (low capillary number) another regime appears, dominated by evaporation. In this evaporative regime, the thickness of the deposit is inversely proportional to the substrate velocity. This scaling was first reported by Dimitrov and Nagayama [9] in 1996 for experiments with colloidal suspensions. These authors also proposed a simple model based on mass balances of both the solution and the solute, which shows that the particles flux inside the meniscus is mainly driven by evaporation. Experiments were extended more recently to other systems [10-12] where the same scaling was observed. The existence of a cross-over between an evaporative regime and a Landau-Levich regime was theoretically predicted by Berteloot et al. [13] (despite the fact that their model did not give the right scaling in the evaporative regime), and experimentally observed by Le Berre et al [10] and Faustini et al [12]. For some configurations a stick-slip motion of the contact line is obtained and leads to regular stripe patterns. This phenomenon has been first mentioned by Adachi and co-authors [14] for colloids and sessile droplet geometry. One remarkable aspect of stick-slip phenomenon is its universality, in the sense that it can be observed for very different systems such as small molecules, colloidal suspensions, polymer solutions, etc (cf for instance [10,15-18] and the recent review by Han and Lin [19]). However the conditions required for strong stick-slip depend on both the process parameters and the physico-chemical properties of the solution, in a non trivial way. The purpose of this paper is to illustrate this

dependence. The first study concerns the influence of the system pH on patterning, for aqueous silica suspensions. The second study is dedicated to the comparison of silica suspensions and polymer solutions.

2. Experiment

2.1 Setup:

The setup principle is similar to classical dip-coating. In dip-coating the substrate is withdrawn from a reservoir which contains coating materials, while in our setup the substrate is motionless and the solution is pumped out from the reservoir. Figure 1 shows a picture of the experimental setup: a sandwich device made of two paralleled glass plates separated by 1mm spacers is vertically immersed into a reservoir which contains the colloidal suspension. The small spacers are located at the top of the glass slides and close to the edges. Due to the 1mm-thin gap, there is a spontaneous capillary rise. This value of the gap is a compromise. It was chosen to get a significant capillary rise while being able to ensure a good parallelism between the two plates. The flow rate of the pumping system controls the contact line velocity V.

The setup is put inside a chamber of volume 60L, where temperature and humidity are regulated by a PID system. In all the experiments presented in this paper, the temperature set-point is 25℃ and the humidity set-point is 30%. A fan blows an air flow to the meniscus through a vertical channel carefully screwed on the top of the two plates. The air flow velocity is chosen to get a uniform evaporation rate but a negligible deformation due to the pressure increase above the meniscus. The gap between the two plates being open, the air escapes through the lateral sides. Note that the air flow may then be different from a classical dip-coating configuration. However, as stated by the simple model of Dimitrov and Nagayama [9] and confirmed by previous simulations [20], the accumulation of non volatile solute at the contact line in our set-up or in dip-coating (but unlike droplets) depends on the total evaporation flux over the meniscus and not on its local density. Then the results can be easily extended to dip coating.

To get the evaporation rate v_{evap} corresponding to the experimental conditions mentioned above, previous experiments were performed with pure water, by cutting the connection between the plates and the reservoir and measuring the decrease of the water level between the two plates.

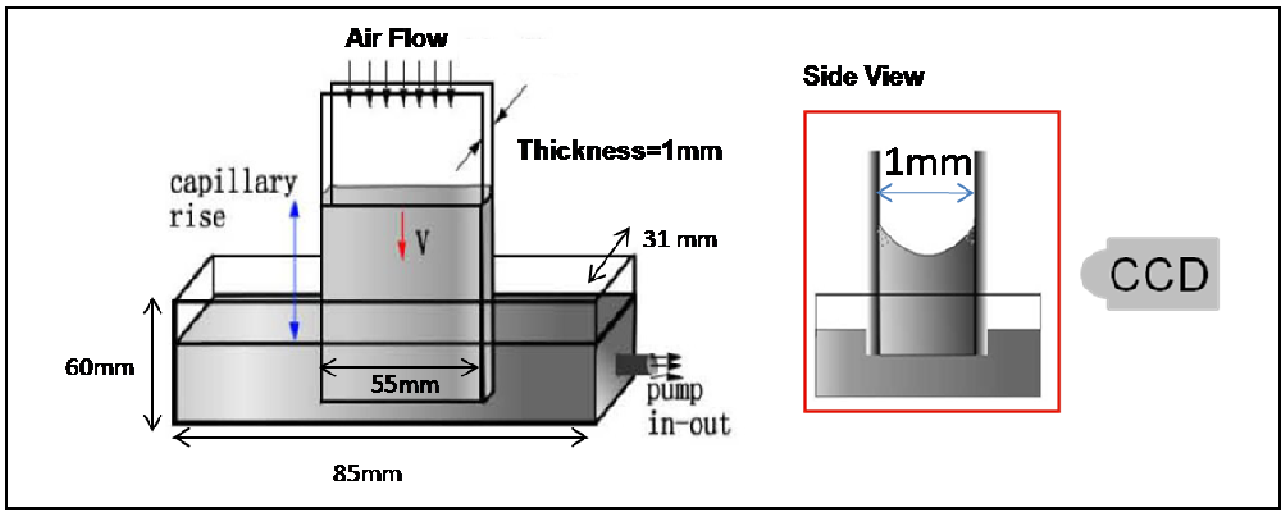

Figure 1 Scheme of the experimental setup.

2.2 Colloidal suspension and polymer solution

Commercial silica suspensions in water have been used (Klebosol from AZ materials, 50R50 wt=50%). Particle mean size is 83nm (standard deviation 7nm) measured by AFM. To prepare the desired concentrations, the industrial solution is diluted in pure water. Corresponding pH is about 9. A smaller pH buffer (pH≈2) is also used to modify the electrostatic interactions between the

particles. This buffer is prepared by diluting Nitric Acid (Sigma-Aldrich 438073) in pure water. All the suspensions are stirred for one hour at room temperature before the experiment starts. For the polymer solution, polyacrylamide (PAAm)/water solutions have been used (Sigma-Aldrich 43,494-9, wt=50%, Mw = 22,4kg/mol, Mw/Mn= 3,5, see [21] for thermodynamic properties). All the polymer solutions are stirred for one night and filtered just before the experiment.

2.3 Experimental protocol

Glass plates are cleaned in “Piranha” solution for 20 minutes (mixture of hydrogen peroxide and sulfuric acid with volume ratio of 0.3/0.7). After rinsing with pure water, plates are dried by nitrogen flow. Just after this cleaning procedure the glass slides exhibit a total wetting by water. Then the glass plates are transferred into the setup and the experiment begins about 15 minutes after. After this delay, the receding contact angle is about 10°, probably due to uncontrolled contamination of the surface. For all the experiments reported in this article, the contact line is receding. Just after filling the tank, a small but fast pumping out of the reservoir is imposed, so that the contact angle at the receding contact line reaches its static receding value.

2.4 Observations:

We record the movement of the meniscus that is on the top of the capillary rise during all the experiment by a CCD camera (AVT Marlin F201B, resolution 1280 x 1024 pixel, Nikkor lens 60 mm f/2.8D). Due to set-up limitations, the camera recording does not provide the absolute value of the capillary rise, but the displacement is known very accurately. Indeed a sub pixel analysis is performed, and leads to a precision of the order of 2 µm for the contact line displacement. Images are analyzed by Igor software. The dried deposits are characterized by profilemetry (Microsurf 3D optical profiler from FOGALE nanotech).

3. Results and discussion

3.1 Stick-slip motion description

By image processing, we can plot the contact line displacement versus time. Figure 2 shows a typical example of a periodic motion, leading to ordered strip patterns parallel to the contact line. For brevity it is called stick-slip motion in the following, even if it does not correspond to a perfect pinning of the contact line. This “pseudo-pinning” has been reported by Moffat and Sefiane [22] for sessile droplets. In this study, stick means that the contact line slows down compared to the mean velocity and slip means that it accelerates. For the two stages (stick and slip), we can deduce the length, velocity and duration from the observation of the contact line displacement. Definitions are straightforward from the diagram drawn in Figure 2:

$\delta h_{stick} = h_2-h_1$, $\delta h_{slip} = h_3-h_2$, $V_{stick} = \delta h_{stick}/(t_2-t_1)$, $V_{slip} = \delta h_{slip}/(t_3-t_2)$, $\delta h_{tot} = \delta h_{stick} + \delta h_{slip}$

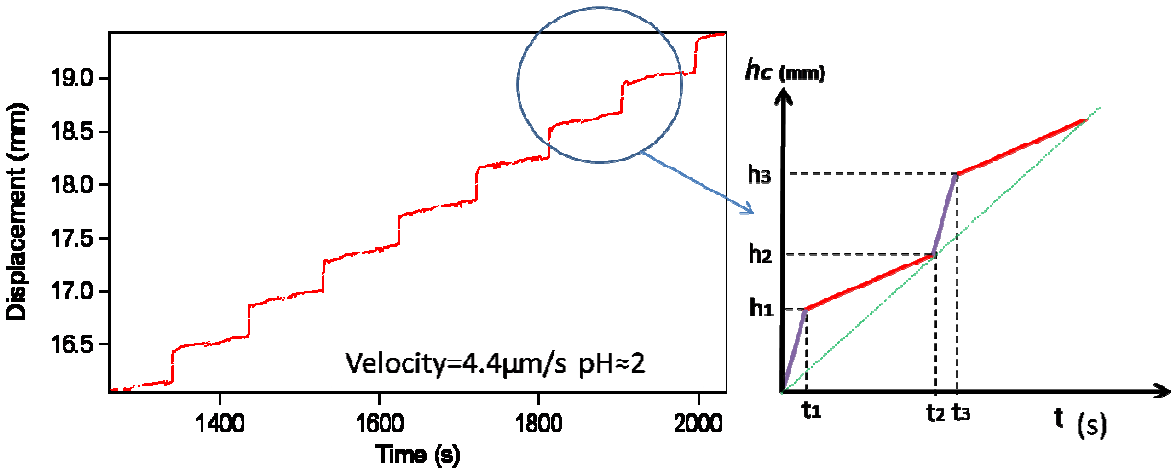

Figure 2: Stick-slip: typical contact line displacement as a function of times for the silica suspension. Left figure corresponds to an experience performed with receding velocity V≈4.4µm/s, evaporation rate v_{evap}≈0.4µm/s, initial volume fraction Φ≈8% and pH≈2. The right figure is a sketch of stick-slip motion definition.

3.2 Silica suspensions: Contact line dynamics and deposit morphologies

The first comparison concerns the influence of the solution pH for silica suspensions. Based on previous results [16-18], the process parameters have been chosen in a range where stick-slip is expected. Two experiments have been performed with the same parameters: receding velocity V≈10µm/s, evaporation rate v_{evap}≈0.4µm/s and initial volume fraction Φ≈8%. The only difference is the pH value of the solutions. Changing the electrostatic interaction between the particles through the pH affects the deposit morphologies significantly, as illustrated in Figure 3. As can be seen from profilometric profiles of the dried deposits, the cross section obtained with pH 9 has smoother contour, longer wavelength, and quite symmetric shape. For pH 2, the deposit is much sharper at one side. The relative contact line displacement, h(t)-Vt, is given in Figure 4 for the two experiments. Average values of the wavelength (δh_{tot}), stick and slip velocities are listed in table 1.

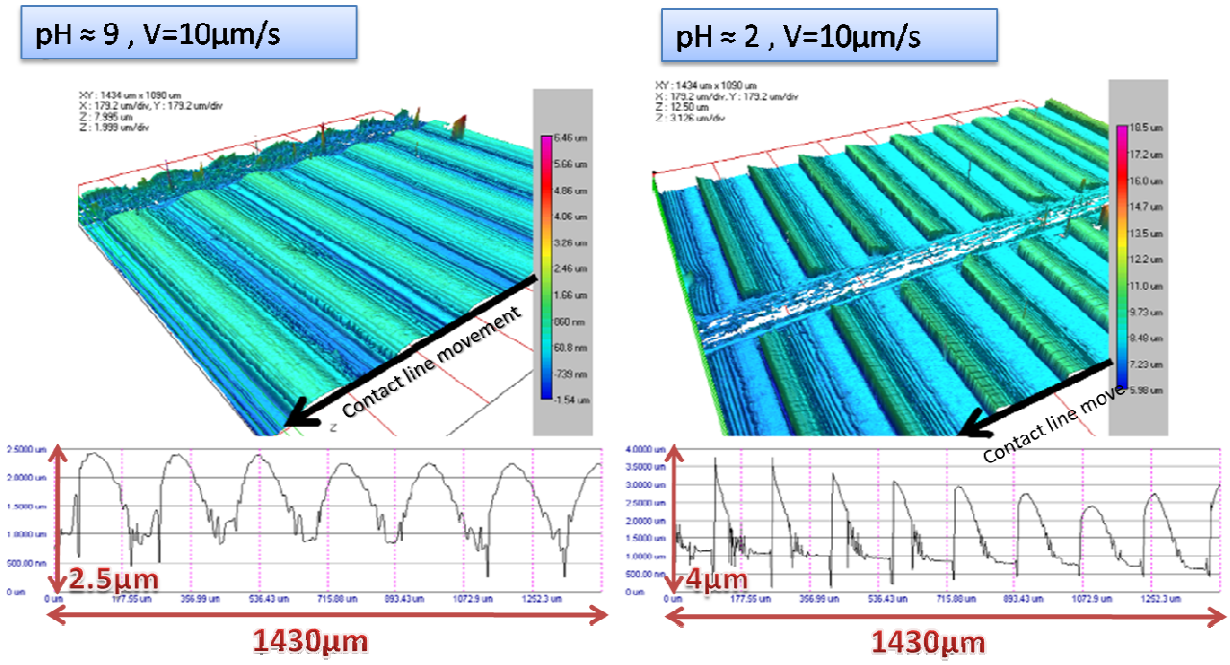

Figure 3. 3D images obtained from profilemeter measurement of the colloidal depositions for different pH values. The plots at the bottom give the thickness profiles, i.e. the cross section of the stripes.

The ratio V_{slip}/V_{stick} is two times larger for pH 2 than for pH 9, which results in the large asymmetry observed on the dried deposit. The slip and stick lengths are smaller for pH 2, and so is the total wavelength. However the mean amplitude is close for the two samples, 1.5 ± 0.1 µm and 1.6 ± 0.2 µm for pH 9 and 2, respectively. Other experiments were performed by changing the substrate velocity V and the same conclusions were obtained. Summary of the results for these two pH and different substrate velocities is given in Figure 5. Data from Bodiguel et al. [17] suggest $v_{ev}\Phi/V$ to be a relevant scaling, so that it was also used in this study. Despite the dispersion of the results, wavelengths obtained at low pH are clearly smaller which confirms the influence of particle interaction forces on the final deposit.

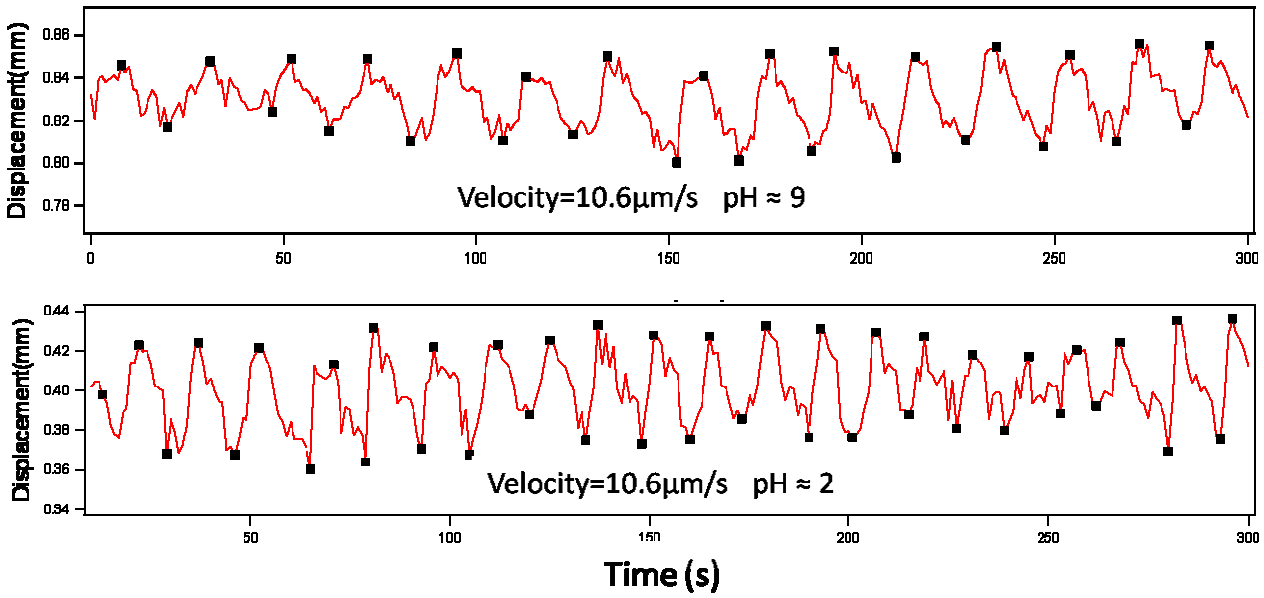

Figure 4: Relative contact line displacement at two different pH values. Upper one corresponds to pH 9, lower one to pH 2.

pH	δh_{stick} (µm)	δh_{slip}(µm)	δh_{tot}(µm)	V_{stick}(µm/s)	V_{slip}(µm/s)	V_{slip}/V_{stick}
≈9	94	111	205	7	16	2.3
≈2	47	98	145	5	23	4.6

Table 1. Stick-slip characteristics for pH 2 and pH 9 suspensions.

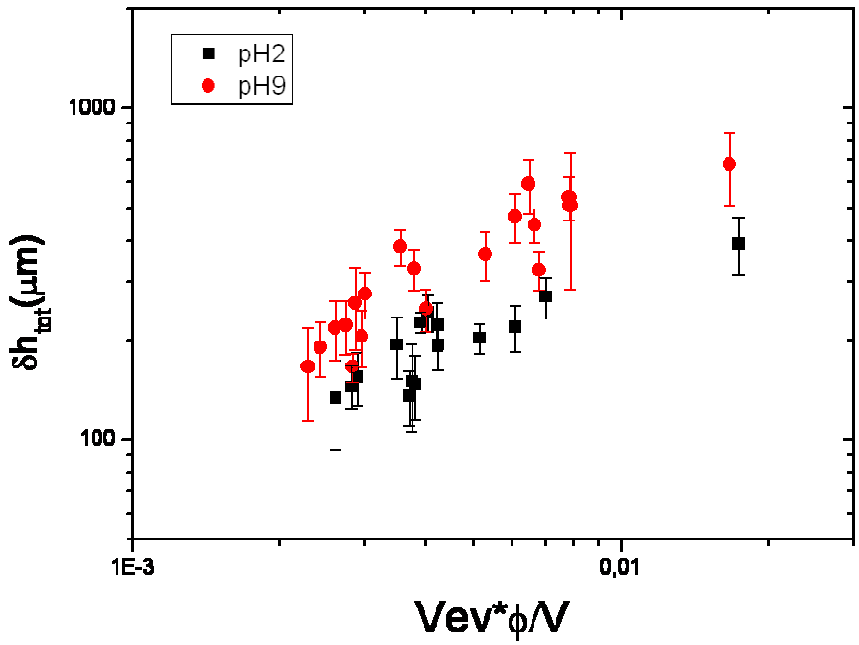

Figure 5. Wavelength as a function of the non dimensional variable $v_{ev}\Phi/V$. (Φ = 8%, 0.31µm/s < v_{ev}<0.58µm/s, 2.2µm/s< V<12.5µm/s)

3.3 Comparison with polymer solution

Experiments are repeated with PAAm polymer solution at 25℃. Close parameters are chosen for the two systems V = 5.2 µm/s, v_{evap}=0.38 µm/s, Φ = 3% for the colloidal suspension, while V = 5.9 µm/s, v_{evap}=0.3 µm/s, Φ = 3.4% for the polymer solution.

For the colloidal suspension, results are similar to the experiments of the previous section at pH 9: we get a clear stick-slip phenomenon. The amplitude of stripe patterns is about 1.5 µm and their shape is symmetric (Figure 6 and 7, left). A very different morphology is obtained for the polymer solution: the dry film is almost flat, with only small and intermittent undulations shown in Figure 6 and 7 (right). The amplitude of these undulations is of order of 20 nm that is two orders of magnitude smaller than for the colloidal suspension. Here undulations are small compared to the whole thickness, so that it is meaningful to define a mean thickness of the dry film. As stated by a previous study [11], it is expected to be of the order of $h_{dry} \approx L\Phi v_{ev}/V$, with L≈330µm that is h_{dry}≈0.6 µm. This is in agreement with the experimental thickness of 0.5 µm measured from profilometry measurement.

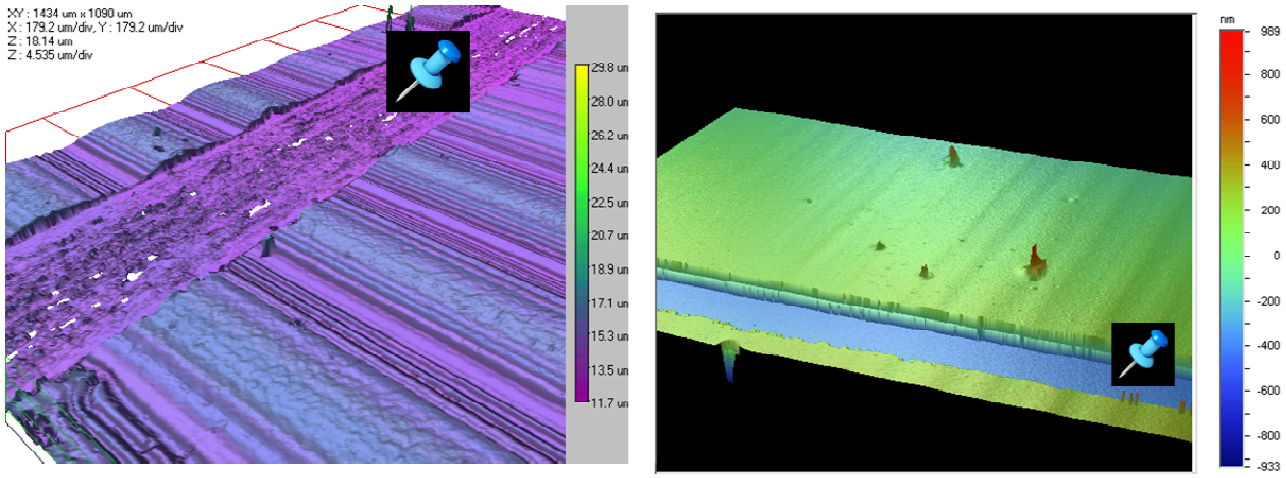

Figure 6: 3D images obtained from profilemeter measurement of the colloidal (left) and polymer (right) deposits. The artificial groove has been made a posteriori on the dry film to estimate the thickness of the film.

Varying the initial volume fraction (2% < ϕ < 7%) or the substrate velocity (0.5 µm/s < V < 500 µm/s), no stick slip was obtained for PAAm solution at room temperature and humidity 30%. It is only by decreasing the polymer volume fraction below 1.5%, or by shifting to higher evaporation temperature that regular stick-slip behavior was again observed. From these first results, it can be drawn that stick-slip occurrence depends on system properties and external parameters (substrate velocity, evaporation rate) in a non trivial way.

Understanding this coupling and the mechanism that drives up the periodic movement of the contact line is still an open question and, as far as the authors know, no general theory is currently available to explain it. In the light of these experimental results, one promising track should be to try to obtain a periodic regime with an hydrodynamic model, as it has already been done for ultra-thin films [23]. For instance the viscosity dependence with solute concentration is known to be very sensitive to the nature of the solute (polymers/colloids) but also to the medium (salt concentration or pH) since it affects particles interaction (see for instance [24]), and to the temperature since it

affects polymer mobility. Next step will then require the detailed characterization of the systems as well as the development of the model to go further in the understanding of patterning.

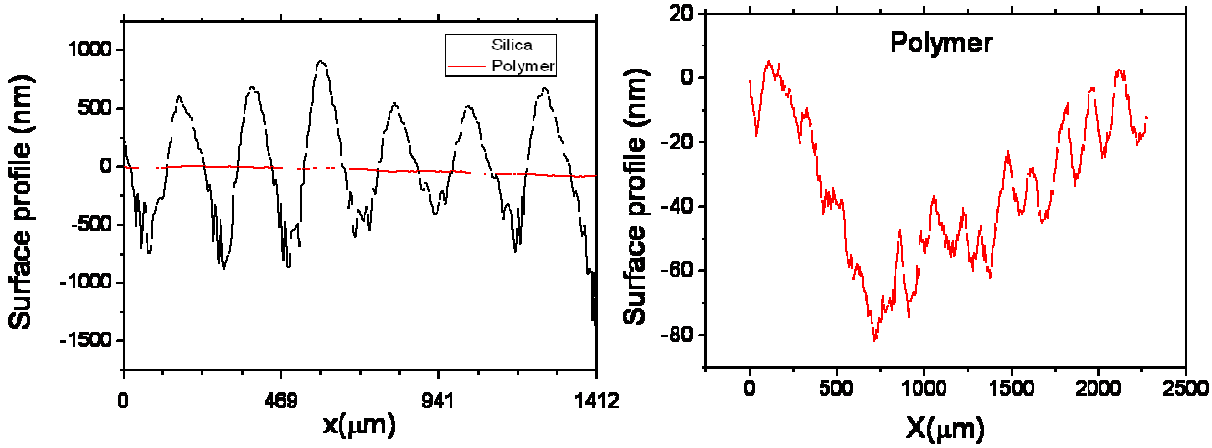

Figure 7: Cross section of the deposits (the origin of the ordinate axis is arbitrary). Left: comparison of colloidal and polymer pattern amplitude. Right: Polymer surface undulations (zoom).

4. Conclusion:

For low capillary numbers, we have studied the stick-slip motion of colloidal systems when drying drives convective self-assembly. The results show that with different pH values, we obtain different wavelengths and morphologies. Under the same conditions, dried polymer films are almost flat with only small undulations on the surface. These experimental results are a fisrt step for better understanding the deposit formation. They will be used to test models currently under investigation.

5. Acknowledgements

We gratefully thank A. Aubertin, L. Auffray, R. Pidoux and C. Borget (FAST Laboratory) for technical support. Deposit images were performed by FOGALE optical profilometer in laboratory ”Sciences et Ingénierie de la Matière Molle” in ESPCI (France). This work was supported by the Marie Curie Initial Training Network: Multiscale complex fluid flows and interfacial phenomena (MULTIFLOW); and Junta de Andalucia (project P07-FQM-02517).

References

[1]M. Ghosh, F. Fan, K. J. Stebe *Langmuir* **23**, 2180-2183 (2007)

[2]K. Ariga, J. P. Hill, M. V. Lee, A. Vinu, R. Charvet, S. Acharya *Sci. Technol. Adv. Mater.* **9**, 014109 (2008)

[3]S. Watanabe, K. Inukai, S. Mizuta, M. T. Miyahara *Langmuir* **25**, 7287–7295 (2009)

[4]R. D. Deegan, O. Bakajin, T. F. Dupont, G. Huber, S. R. Nagel, T. A. Witten, *Nature* **389,** 827–829 (1997)

[5]W. D. Ristenpart, P. G. Kim, C. Domingues, J. Wan, H. A. Stone, *Phy. Rev. Let*. **99**, 234502 (2007)

[6]I. I. Smalyukh, O. V. Zribi, J. C. Butler, O. D. Lavrentovich, G. C. L. Wong *Phy. Rev. Let.* **96**, 177801 (2006)

[7] L. Landau, B. Levich, *B. Acta Physicochem. USSR,* **17**, 42–54 (1942)

[8] B. Derjaguin, *B. Acta Physicochim. USSR,* **20**, 349 (1943)

[9] A.S. Dimitrov, K. Nagayama, *Langmuir* **12**, 1303-1311 (1996)

[10]M. Le Berre, Y. Chen, D. Baigl *Langmuir* **25,** 2554-2557 (2009)

[11] G. Jing, H. Bodiguel, F. Doumenc, E. Sultan, B. Guerrier *Langmuir* **26**, 4, 2288-2293 (2010)

[12] M. Faustini, B. Louis, P. A. Albouy, M. Kuemmel, D. Grosso *J. Phys. Chem. C* **114***,* 7637–7645 (2010)

[13] G. Berteloot, C. Pham, A. Daerr, F. Lequeux, L. Limat, *Europhys. Lett*., **83**, 14003 (2008)

[14] E. Adachi, A.S. Dimitrov, K. Nagayama *Langmuir*, **11**, 1057–1060 (1995).

[15] J. Xu, J. Xia, S. Won Hong, Z. Lin, F. Qiu, Y. Yang, *Phy. Rev. Let.* **96**, 066104 (2006)

[16] H.Bodiguel, F.Doumenc, B.Guerrier *EPJ-ST* **166**, 29-32 (2009)

[17] H. Bodiguel, F. Doumenc, B. Guerrier *Langmuir* **26**, 13, 10758-10763 (2010)

[18] H. Bodiguel, F. Doumenc, B. Guerrier, Erratum of [17], *Langmuir* **27**, 13, 13352 (2011)

[19] W. Han, Z. Lin *Angew. Chem., Int. Ed.* **51**, 7, 1521-3733 (2012)

[20] F. Doumenc, B. Guerrier *Langmuir* **26**,13, 10758-10763 (2010)

[21] D. Alonso de Mezquia, F. Doumenc, M. Mounir Bou-Ali *J. Chem. Eng. Data,* **57**, 776-783 (2012).

[22] J.R. Moffat, K.Sefiane, M.E.R. Shanahan, *J. Phys. Chem. B*, **113**, 26, 8860-8866 (2009)

[23] L. Frastia, A.J. Archer, U. Thiele, *Phys. Rev. Lett*., 106, 077801 (2011)

[24] C. Allain, M. Cloitre, B. Lacoste, M. Marsone, *J. Chem. Phys*, 100, 4537 (1994)